Postharvest Biology and Technology 219 (2025) 113250

Contents lists available at ScienceDirect

Postharvest Biology and Technology

journal homepage: www.elsevier.com/locate/postharvbio

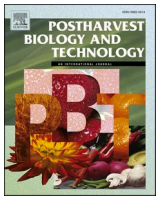

Ethylene mitigates nut decay and improves nut quality of *Torreya grandis* during postharvest by changing microbial community composition

Jinwei Suo [a,b,1], Zhanhua Zhou [a,b,1], Mohamed A. Farag [c], Zuying Zhang [a,b], Jiasheng Wu [a,b,*], Yuanyuan Hu [a,b,*], Lili Song [a,b,*]

[a] State Key Laboratory of Subtropical Silviculture, Zhejiang A&F University, Lin'an, Zhejiang Province 311300, China
[b] Sino-Australia Plant Cell Wall Research Centre, School of Forestry and Biotechnology, Zhejiang A&F University, Lin'an, Zhejiang Province 311300, China
[c] Pharmacognosy Department, College of Pharmacy, Cairo University, Kasr el Aini st., Cairo P.B. 11562, Egypt

ARTICLE INFO

Keywords:
Ethephon
Post-ripening stage
Nut nutritional quality
Enzyme activity
High-through sequencing

ABSTRACT

Torreya grandis nuts require postharvest ripening for oil accumulation, with ethephon (ETH) commonly used to induce such process, thereby impacting the endophytic microbial community. In this study, shelled *T. grandis* nuts were divided into two groups: one treated ETH and the other with water (CK). The ETH treatment expedited nutrient metabolism from day 5 till day 10 as manifested by a decline in starch content, while increasing oil and soluble protein, enhancing enzyme activity, and reducing nut decay incidence. ETH-treated nut exhibited greater bacterial and fungal diversity compared with CK, along with more distinct microbial biomarkers. Structural equation modeling linked with ETH treatment revealed that increased oil content was mediated via increased abundance of *Myxozyma*, *Rhodobacter*, and pyruvate kinase activity. *Chalara*, a fungal biomarker, was strongly correlated with decay incidence. These findings offer valuable biomarkers for mitigating decay and improving *T. grandis* nuts quality during post-ripening stage in the future.

1. Introduction

Torreya grandis nuts are a rarity in China and are highly regarded for their exceptional flavor, rich nutrient content, high oil level, and myriads of bioactive compounds (Wu et al., 2018; Suo et al., 2019). In *T. grandis*, the postharvest ripening process is essential for oil formation and flavor development in *T. grandis* nuts (Hu et al., 2022). Numerous studies have indicated that various microorganisms present in postharvest fruit or nuts can act to influence the quality and shelf life of the product (Shi et al., 2021; Zhimo et al., 2021; Huang et al., 2024). Concomitantly, *T. grandis* nuts are susceptible to decay during the post-harvest stage, leading to economic losses (Li and Dai, 2007). However, our understanding of the mechanisms governing nut quality, particularly regarding changes in microbial community in *T. grandis* nuts, remains incomplete.

Microorganisms play pivotal roles in fruit growth, postharvest and storage, encompassing beneficial, pathogenic and spoilage microorganisms (Wassermann et al., 2019; Shi et al., 2021; Lane et al., 2024). Beneficial microbes influence nuts quality by directly affecting nutrients' level (Aguilar et al., 2007; Wang et al., 2011; Bourdichon et al., 2012). Yu et al. (2021) reported that genera *Acetobacter* and *Gluconobacter* was linked to increased sweetness while reducing acidity in Chinese bayberry. Moreover, beneficial fungal communities demonstrated positive correlation with starch content, peroxidase, and polyphenol oxidase activities (Li et al., 2022). Xie et al. (2021) identified a positive correlation between ripening metabolism and certain endophytes during the postharvest process of kiwifruit (*Actinidia chinrnsis*), including *Enterococcus, Vishniacozyma_victoriae, and Epicoccum_nigrumand*. All these results indicate that changes in microbial community could be associated with changes in flavor and nutrients composition in fruit which has yet to be tested in the case of *T. grandis* nut. Comparative analysis between healthy and unhealthy fruit showed that genes in the microbiome associated with defense mechanisms had higher relative abundances in healthy fruit, whereas microbes in diseased fruit were engaged in energy conversion and carbohydrates digestion (Wu et al., 2019). The growth patterns of *Botryosphaeira* and *Penicillium* indicated an increase in their abundance over storage time, leading to continuous fruit decay (Zhang et al., 2021a). Additionally, Li et al. (2022) revealed

* Corresponding authors at: State Key Laboratory of Subtropical Silviculture, Zhejiang A&F University, Lin'an, Zhejiang Province 311300, China.
E-mail addresses: wujs@zafu.edu.cn (J. Wu), hyy_1985@zafu.edu.cn (Y. Hu), lilisong@zafu.edu.cn (L. Song).
[1] These authors have contributed equally to this work.

https://doi.org/10.1016/j.postharvbio.2024.113250
Received 4 August 2024; Received in revised form 23 September 2024; Accepted 7 October 2024

that *Botryosphaeira*, *Neofusicoccum* and *Colletotrichum* were associated with chestnut (*Castanea sativa*) decay during storage, becoming dominant species later in the storage period. Consequently, investigating the diversity and composition of the microbiota community during the post-harvest ripening stage of *T. grandis* nuts and its relationship with nut quality holds significant potential value for fruit improvement.

Ethylene possesses the ability to stimulate and accelerate the post-harvest period, expediting and homogenizing fruit ripening (Tovar et al., 2011; Han et al., 2024). Maduwanthi and Marapana (2021) revealed that ETH influenced banana firmness and total sugars, albeit causing *ca.* 50 % loss of vitamin C level at the ripening stage. ETH treatment can impact fruit quality by altering microbiome metabolism. For example, ethylene micro-environment promoted the physiological ripening of kiwifruit (*Actinidia chinrnsis*), which is associated with dynamic variations in three bacterial genera and 6 fungal species during postharvest (Xie et al., 2021). It has been reported that ethylene exerted an inhibitory effect on aflatoxins contamination in raw peanuts due to its strong inhibition of *Aspergillus parasiticus* growth (Roze et al., 2004). Our previous study demonstrated that ethylene treatment increased amino acids level, especially umami amino acids (Zhang et al., 2022). However, there is limited information on the effect of ethylene on *T. grandis* nuts regarding nutrients conversion and changes in microbial community.

Consequently, main objective of this study was to compare two post-harvest treatments for *T. grandis* nuts, the control group (CK) and the ethephon (ETH) group. Specifically, our aims were (1) to reveal dynamic changes in nut quality (e.g., nut nutrient, decay incidence) with post ETH treatment; (2) to determine changes in microbial structure through 16S and ITS sequencing; (3) to clarify the interaction between microbiome communities and nut quality in ethylene-treated *T. grandis* nuts during the post-ripening stage. The results provided better insight into relationship between microbial communities and *T. granids* nut quality, thereby aiding in the identification of potential biological control measures for improving quality in *T. grandis* nut kernels during the post-ripening stage.

2. Materials and methods

2.1. Plant materials and treatment

The cracked *T. grandis* cv. 'Merrillii' nuts were manually harvested at the aril cracking stage from a commercial orchard in Zhuji City, Zhejiang province, China, in September 2021. Within 4 hours of harvesting, fruit were transported to our laboratory, where the aril-covered nuts were manually removed. The nuts with hard shell of free visible mechanical damage and uniform size (about 27.2 ± 1.7 mm length) were selected for further study. The selected nuts were washed with clean water and left to air dry at room temperature (25 ℃) for 5 h until no visible external moisture was observed. After that, *ca.* 96 kg of nuts were randomly divided into two groups: ETH group, where nuts (*ca.* 4 kg) were sprayed with a 50 mL of 4000 mg·L^{-1} ethephon solution (Shanghai yuanye Bio-Technology Co., Ltd), which corresponded to an ethylene gas concentration of 969 μL·L^{-1}. The CK group was sprayed with 50 mL distilled water. Both ETH and CK group were placed in a sealed storage box (80 cm in length, 40 cm in width, and 15 cm in height) and incubated for 24 h. Subsequently, both groups were then maintained at 25 ℃ and 90 % relative humidity during the post-ripening stage. The concentration of ETH and processing environment were chosen in accordance with the preliminary experimental results (Zhang et al., 2020; Suo et al., 2022). For each group, three biological replicates were randomly selected and sampled at 4 storage time intervals (0, 5, 10 and 15 days). Kernel samples were stored at −80 ℃ for subsequent DNA extraction, and frozen nut tissues were used for nutrients and key enzymatic activity assays.

2.2. Determination of nut quality

The nut quality changes, such as oil, starch, soluble sugar and soluble protein contents, were assessed at 4-day interval expressed as g kg^{-1} on a fresh weight basis. The crude oil mixture was extracted from nuts using Soxhlet apparatus as described by García-Ayuso et al. (2000). The mixture was then dried overnight in a fume hood to obtain the residue, which was subsequently weighed to determine oil content. The nut residue sample left after oil extraction was used to determine soluble sugars and starch content using the anthrone reagent colorimetric method (Zheng, 2006). The soluble protein content was measured according to Coomassie Brilliant blue G-250 method (Read and Northcote, 1981), using bovine serum albumin as a standard. Three biological replicates were used for the determination of each parameter.

The calculation method for the conversion completion rate of oil, soluble protein, and soluble sugar was as follows: the value at each measurement points minus the minimum value during post-ripening stage, then divided by the difference between the maximum value and the minimum value. For starch complete rate, the value at each measurement point during the post-ripening stage was subtracted from the value at day 0, and then divided by the difference between the maximum and minimum values.

2.3. Determination of key enzyme activities in nuts

The activities of the enzymes amylase (α-amylase and β-amylase, which catalyze the decomposition of starch in the nut), pyruvate kinase (PK, an important enzyme in the glycolytic pathway that also provides carbon skeletons for fatty acid biosynthesis), diacylglycerol acyltransferase (DGAT, catalyzes the terminal reaction in triglyceride synthesis), sucrose synthase and sucrose phosphate synthase (SUS and SPS, key enzymes in sugar metabolism), and transaminase (which catalyzes the reversible transfer of an amino group from an amino donor to an aldehyde, prochiral keto acid, or ketone, resulting in a amine) were measured using enzyme-linked immunosorbent assay (ELISA) kits according to the manufacturer's protocols (Jiangsu Meimian Industrial Co., Ltd, China). One unit of α-amylase activity is defined as the amount of enzyme required to hydrolyze 1 mL of 2 % soluble starch per hour at 25°C, expressed as 10^3 U kg^{-1}. One unit of β-amylase activity is defined as the amount of enzyme required to produce 1 mg of maltose per hour from 2 % soluble starch under the same conditions, also expressed as 10^3 U kg^{-1}. One unit of PK activity is defined as the amount of enzyme required to convert 1 μM of phosphoenolpyruvate (PEP) into pyruvate per minute under conditions of pH 7.4 and 25°C, expressed as 10^3 U kg^{-1}. One unit of DGAT activity is defined as the amount of enzyme required to catalyze the formation of 1 mg of triacylglycerol from diacylglycerol and fatty acyl groups per hour at 37°C, expressed as 10^3 U kg^{-1}. One unit of SUS or SPS activity is defined as the amount of enzyme required to catalyze the production of 1 μg of sucrose per gram of sample per minute at 37°C, expressed as 10^3 U kg^{-1}. One unit of transaminase activity is defined as the amount of enzyme needed to produce 1 μM of amino acid per hour at 25°C, expressed as 10^3 U kg^{-1}. Each enzyme activity was determined using three biological replicates, with results expressed on a fresh weight basis.

2.4. Decay incidence

The decayed nuts were soft to the touch, with creamy yellow color and smelly, and the seed coat was very dark black. Decay incidence was calculated by the number of infected nuts dividing by the total number of *T. grandis* nut in each replicate. Fifty nuts were randomly selected for analysis every 5 days. Data were averaged from three biological replicates.

$$\text{Decay incidence (\%)} = \frac{\text{number of decayed nuts}}{\text{total number of nuts}} \times 100$$

2.5. DNA extraction, PCR amplification and sequencing

A kit was used for DNA extraction from 500 mg of homogenized kernel using the Fast DNA Spin Kit for Soil (Merck KGaA, Darmstadt, Germany). Each treatment at each time point was composed of three replicates, and each replicate encompassed 20 nuts. The bacterial 16S rRNA and fungal ITS genes were amplified using primer pairs of 799 F/ 1193 R (Xie et al., 2021) and ITS1F/ ITS2R (Zhang et al., 2021a), respectively. PCR reactions were run to generate the 16S amplicons in a total volume of 20 μL, containing 10 μL of 2×Pro Taq, 08 μL of each primer (5 μM), 10 ng μL^{-1} of DNA template, and finally nuclease-free water up to 20 μL. PCR reactions used to generate the ITS amplicons were also conducted in a total volume of 20 μL, containing 2 μL of 10×buffer, 2 μL of 2.5 mM dNTPs, 0.8 μL of each primer (5 μM), 0.2 μL of rTaq polymerase, 0.2 μL of BSA, 10 ng of DNA template, and 4 μL of nuclease- free water. PCR cycle for both organisms was performed using the following program: 3 min at 95 ℃ for initial denaturation, followed by 13 cycles (bacteria) or 35 cycles (fungi), at 95 ℃ for 30 s, annealing at 55 ℃ for 30 s, and elongation at 72 ℃ for 45 s, with the final extension step for 10 min at 72 ℃, and storage at 10 ℃ for infinity. The PCR products were separated on a 2 % agarose gel and sequenced using the Illumina MiSeq 2000 platform (Illumina, San DIiego, USA) according to the standard protocol of Majorbio Bio-pharm Technology Co., Ltd (Shanghai, China).

2.6. Data processing and analysis

The raw ITS and 16S rRNA sequencing reads were demultiplexed and quality-filtered by fastp (https://github.com/OpenGene/fastp, version 0.19.6), and then merged by Flash (https://ccb.jhu.edu/software/FLASH/index.shtml, version 1.2.11). The sequences were clustered into Amplicon Sequence Variants (ASV) at 97 % similarity using UPARSE (http://www.drive5.com/uparse/, version 11). The taxonomy of each ASV representative sequence was analyzed using RDP classifier (http://rdp.cme.msu.edu/, vision 2.13). Five taxa classifications-phylum, class, order, family, genus levels-were analyzed and plotted using QIIME (http://qiime.org/install/index.html, vision 1.9.1) as described by Li et al. (2022).

The α-diversity analysis reflects the abundance and diversity of microbial communities in each treatment during the post-ripening stage, while β-diversity measures the similarity or dissimilarity between two microbial communities. The α diversity (Ace) was performed using mothur (https://www.mothur.org/wiki/Download_mothur, vision 1.30.2). To further determine whether there were differences at the ASV level between the two observed nut samples (CK and ETH group) during the post-ripening stage, bacterial and fungal community compositions were analyzed using principal component analysis (PCA) based on the Anosim (Hu et al., 2021). Taxonomic trees were generated using the metacoder package to identify and visualize overall microorganism abundance (Zhimo et al., 2021). Common ASVs among the 3 times were shown in ternary plot (Tian and Wang, 2020). Linear discriminant analysis effect size (LEfSe) analysis, emphasizing both statistical significance and biological relevance, was used to identify significantly altered bacterial and/or fungal taxonomic groups induced by ETH and post-ripening time using the online Galaxy workflow framework (LDA ≥ 3.5) (http://huttenhower.sph.Harvard.edu/galaxy/) (Tian and Wang, 2020; Yu et al., 2022). The fungal functional group (guild) of each ASV was inferred using FUNGuild (Yang et al., 2023).

2.7. Statistical analysis

Each experiment was performed in three replicates. The significance of the two treatments during the post-ripening stage was conducted using one-way analysis of variance (ANOVA). The effects of ETH and post-ripening time were calculated using a two-way ANOVA without initial samples (0 day). Principal component analysis (PCA) was used to investigate the relative impact of significant ethylene and post-ripening time variables on nut qualities with Origin 2021 software. Using the linkET package, the Mantel test was employed to investigate Spearman's linkages between nut decay incidence and potential fungal pathogens (Sun et al., 2022). A piecewise structural equation model (SEM) was established using the package "piecewise" in R 4.2.3 to determine the direct and indirect effects of time or ETH on nut nutrients through nut microorganism and enzyme activities (Lefcheck, 2015).

3. Results

3.1. Changes in macronutrients and nut decay incidence of T. grandis nuts during the post-ripening stage

In *T. grandis*, starch is degraded into soluble sugar during the post-ripening stage, which provides material and energy for protein and oil synthesis. Indeed, the content of oil, soluble sugar, and soluble protein showed an increasing trend, whereas starch content exhibited a decreasing trend (Fig.S1). Compared to CK group, the ETH group had higher oil content from day 5 till day 10, as well as a higher soluble protein content at day 10 (Fig. S1). The highest levels of oil, soluble sugar, soluble protein, and minimum content of starch showed no significant difference between CK and ETH groups (Fig. 1). The oil complete rate in CK group was 55 % and 79 % at day 5 and day 10, respectively, versus a complete rate in ETH group of 69 % and 91 % at day 5 and day 10, respectively. Similarly, the starch complete rate in CK group was 59 % and 76 % at day 5 and day 10, compared with 64 % 83 % in ETH group. There was no significant difference in oil content between day 10 and day 15 in ETH group, but there was a remarkable variation from that in CK. To further investigate whether there was distinction in nutrients during the post-ripening stage, the responses of the four measured macronutrients in context to the two treatments were analyzed using PCA (Fig. S1E). Nut specimens collected at day 5 and day 10 of ripening time (for both ETH and CK group) were clearly separated from those at day 15, with clear discrimination observed between ETH and CK groups at day 5 and day 10 of the post-ripening stage.

The interior seed coat of *T. grandis* exhibited a dark red color, and the kernels appeared milky white at day 15 of the post-ripening stage (Fig. 1E). However, the seed coat of decayed nuts turned dark black in color, with the kernels becoming soft with creamy yellow (Fig. 1E). In addition, decaying incidence under both CK and ETH treatment remained at lower level from day 0 till day 10 of the ripening time. Subsequently, ETH group exhibited 86 % lower decay than that of CK group at day 15 (Fig. 1F).

3.2. Changes in enzyme activities mediating for nutrients conversion in T. grandis nuts during the post-ripening stage

All nut enzyme activities increased with increasing ripening time (Table 1). Compared with CK, all nut enzymes exhibited higher activities under ETH treatment throughout the entire post-ripening stage. Both factors (ETH and post-ripening time) influenced the activities of α-amylase, β-amylase, SUS, SPS, and transaminase ($P<0.05$). Correlation analysis showed that all nut enzyme activities were negatively correlated with nut starch content, but positively correlated with oil, soluble sugar and soluble protein contents (Fig. S2).

3.3. Microbial compositional differences in T. grandis nut post storage with different treatments

A taxonomic dendrogram revealed the most numerous types of amplicon sequence variant (ASV) classifications of bacteria in CK and ETH groups at the phylum level: Proteobacteria (68 % and 77 %), Firmicutes (15 % and 6 %), Actinobacteriota (8 % and 8 %), and Bacteroidota (6 % and 7 %) (Fig. S3A and S3B). In case of fungi, the most

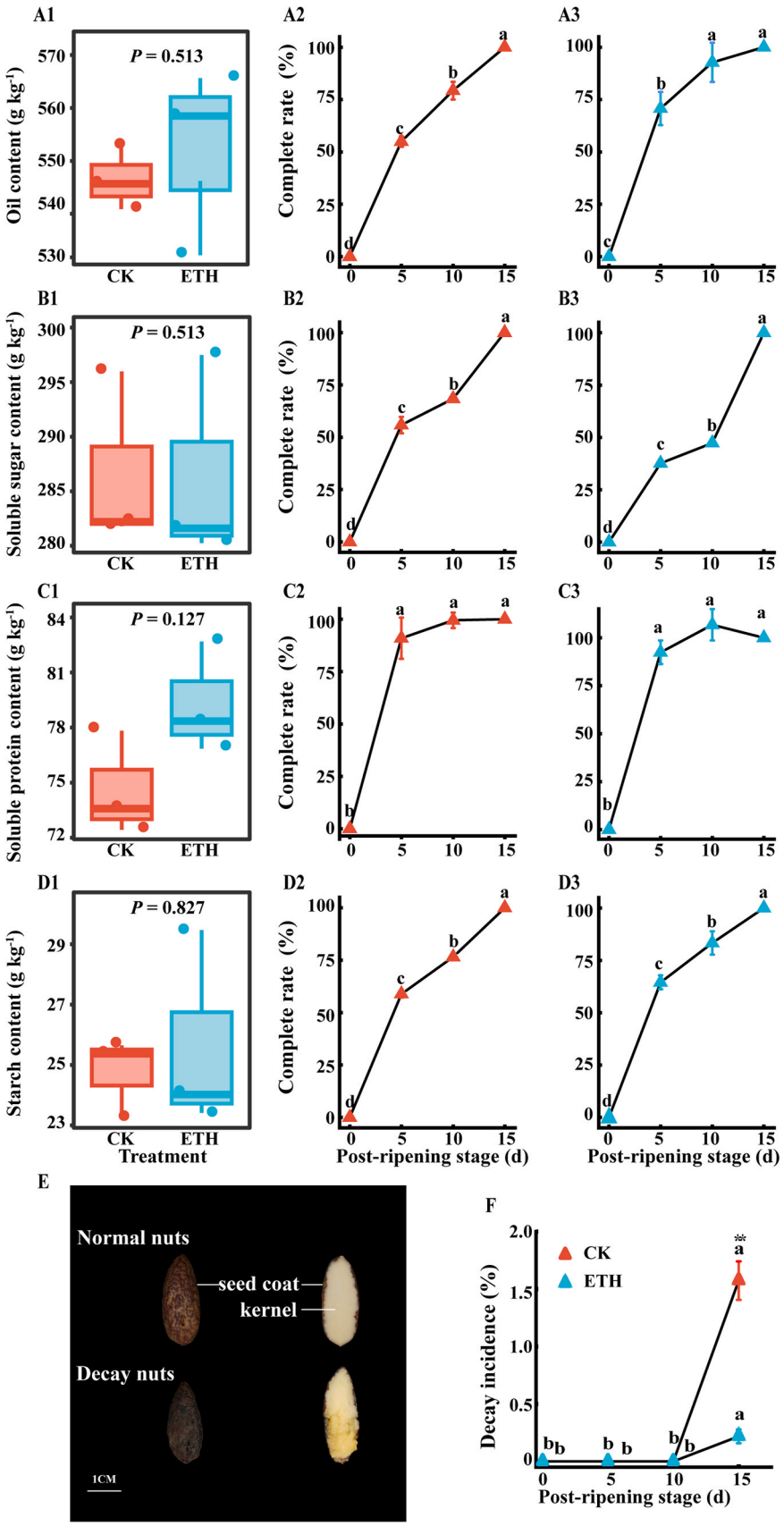

Fig. 1. The maximal levels of oil (A1), soluble sugars (B1), soluble protein (C1), starch (D1), and the completion rate of nutrients conversion under CK (A2-D2) and ETH treatment (A3-D3) during the post-ripening stage, along with a photograph of *Torreya grandis* cv. 'Merrillii' nuts at day 15 of ripening stage (E), and changes in decay incidence (F). Different lowercase letters indicate a significant difference under CK or ETH during the post-ripening stage. Asterisks denote significant differences between CK and ETH at the same post-ripening stage, * $P < 0.05$; ** $P < 0.01$.

Table 1
Effect of ethylene and post-ripening time on nut enzyme activity.

Treatment	Post-ripening time	α-amylase (10^3 U kg^{-1})	β-amylase (10^3 U kg^{-1})	PK (10^3 U kg^{-1})	DGAT (10^3 U kg^{-1})	SUS (10^3 U kg^{-1})	SPS (10^3 U kg^{-1})	transaminase (10^3 U kg^{-1})
CK	0d	40.73±0.74b	24.9±0.4c	136.83±2.84b	14.34±0.31b	31.35±0.22b	14.45±0.19b	56.19±1.47b
	5d	41.37±1.77b*	25.62±0.56bc**	136.23±3.06b*	14.33±0.63b*	30.97±1b**	15.35±0.34ab*	56.42±1.46b
	10d	42.77±1.4ab*	27.46±0.98ab**	152.05±0.43a	14.66±0.42ab*	32.9±0.11ab**	15.93±0.26a**	55.98±1.07b**
	15d	45.81±0.16a*	29.44±0.79a**	142.09±0.04b*	16.02±0.24a	34.71±1.03a**	16.14±0.69a	62.67±0.51a*
ETH	0d	40.73±0.74c	24.9±0.4c	136.83±2.84b	14.34±0.31b	31.35±0.22d	14.45±0.19c	56.19±1.47c
	5d	49.53±1.06b	32.41±0.53b	162.62±7.33a	16.72±0.14a	38.02±0.58c	16.67±0.33b	63.37±2.12b
	10d	53.56±0.28a	33.33±0.69b	168.32±6.51a	17.04±0.39a	40.97±0.81b	18.54±0.24a	66.83±0.73ab
	15d	55.68±1.15a	36.33±0.71a	172.68±5.35a	17.05±0.34a	43.88±0.3a	18.58±0.67a	69.09±1.51a
Time		0.002	0.002	0.001	ns	ns	<0.001	0.023
Treatment		<0.001	<0.001	<0.001	<0.001	<0.001	<0.001	<0.001
Time × Treatment		ns	ns	ns	ns	ns	ns	ns

Note: PK, pyruvate kinase; DGAT, diacylglycerol acyltransferase; SUS, sucrose synthase; SPS, sucrose phosphate synthase. Time, post-ripening time; Treatment, different post-harvest treatments effect; Time × Treatment, post-ripening time × different post-harvest treatments effect. Different letters in the same row indicated the significant difference at P <0.05 level. Asterisks denote significant differences between CK and ETH treatments at same post-ripening time, * $P < 0.05$; ** $P < 0.01$.

abundant phylum was Ascomycota, comprising 96 % and 88 % at CK and ETH treatment, respectively (Fig. S3C and S3D).

To better understand how ETH treatment affected bacteria and fungi composition during ripening-time, generalist or sample-specific bacteria and fungi taxa of each treatment were examined by ternary plots, and the major genera were marked (Fig. 2). Species that were identical and had high relative abundance were targeted to elucidate the microbial changes under either CK or ETH treatment. For bacteria, *Allorhizobium-Neorhizonium-Pararhizobium-Rhizobium*, *Carnimonas*, *Novosphingobium*, *Pseudomonas*, *Rhodobacter*, *Rosenbergiella*, *Stenotrophomonas*, unclassified_f__Comamonadaceae, unclassified_o__Enterobacterales and unclassified_f__Erwiniaceae were found enriched both under CK and ETH treatment during the whole post-ripening stage (Figs. 2A and 2B). In case of fungi, *Arthrobotrys*, *Aspergillus*, *Fusarium*, *Gibberella*, *Lasiodiplodia*, *Myxozyma*, *Ogataea*, and *Zygoascus* were enriched both under CK and ETH treatment during the whole post-ripening stage (Figs. 2C and 2D). The diversity of bacteria and fungi was found greater under ETH treatment compared with CK during the post-ripening stage. Additionally, their distribution appeared to be more uniform across the different time intervals (Fig. 2).

The relative abundance of *Allorhizobium-Neorhizonium-Pararhizobium-Rhizobium*, *Novosphingobium*, *Pseudomonas*, and *Rhodobacter* under CK remained steady from day 0 till day 10, and increased from day 10 till day 15 (Fig. 3A). Both relative abundances of unclassified_o__Enterobacterales and unclassified_f__Erwiniaceae under CK showed an increasing trend from day 0 to day 10, but decreased from day 10 to day 15. Under ETH treatment, the relative abundance of *Allorhizobium-Neorhizonium-Pararhizobium-Rhizobium* increased throughout the entire post-ripening stage (Fig. 3A). *Pseudomonas*, *Rosenbergiella*, and unclassified_f__Erwiniaceae under ETH treatment reached peak relative abundance at day 5, and then showed a decreasing trend from day 10 till day 15. The genus *Carnimonas* under CK showed an increasing trend from day 0 till day 10, but decreased at day 15. In contrast, relative abundance of *Carnimonas* under ETH treatment showed a decreasing trend during the post-ripening stage (Fig. 3A). For fungi, *Fusarium* and *Aspergillus* initially showed an increasing trend followed by a decline as the post-ripening stage progressed (Fig. 3B). Both *Gibberella* and *Lasiodiplodia* showed a decreasing trend from day 0 till day 15 (Fig. 3B). The relative abundance of *Myxozyma* under both CK and ETH treatments increased from day 0 till day 15. Compared with CK, fungal genera *Fusarium*, *Myxozyma*, *Ogataea*, and *Zygoascus* showed higher relative abundance under ETH treatment throughout the entire post-ripening stage.

There appeared to be more bacterial and fungal taxa at various taxonomic levels affected by ETH than CK from day 0 till day 15 (Figs. 3E and 3F). For ETH treatment, specific biomarkers at day 5 of

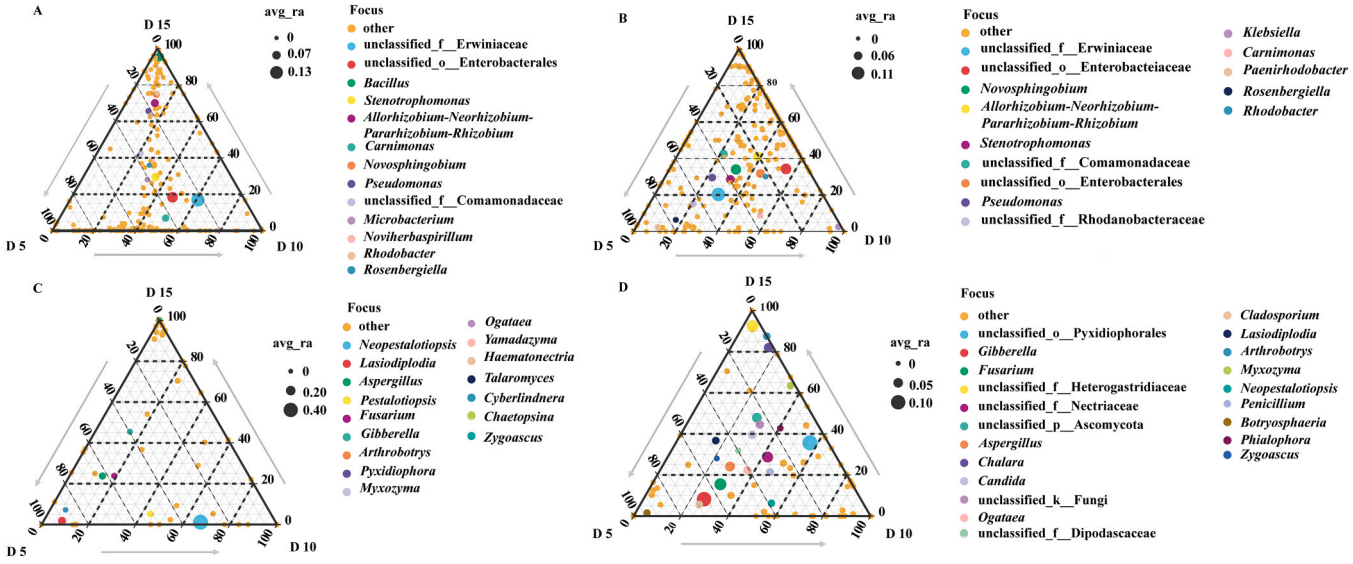

Fig. 2. Ternary plots represented all genera innut samples at different post-ripening times (day 5, day 10, and day 15). Each circle corresponds to one genus, with size representing average relative abundance, and position determined by relative abundance in the corresponding group. A: bacteria under CK. B: bacteria under ETH. C: fungi under CK. D: fungi under ETH.

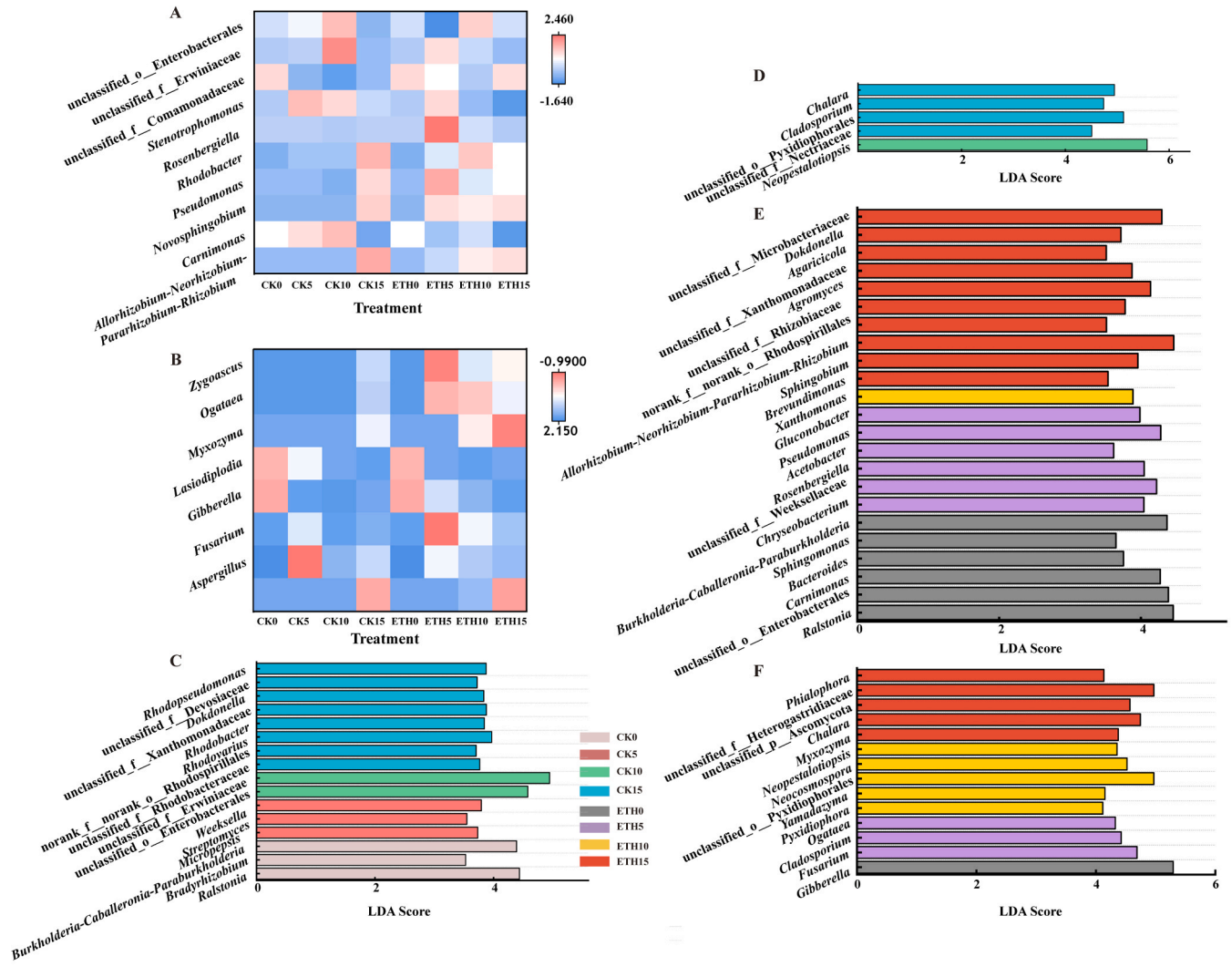

Fig. 3. Heatmap of the relative abundance of bacterial (A) and fungal (B) genus communities (generalist or sample-specific taxa). LEfSe analysis of bacteria (C-D) and fungi (E-F) on days 0, 5, 10, and 15 of nuts under CK and ETH treatments. The LDA score (LDA > 3.5 and P < 0.05) of the biomarker at the genus level is shown in the bar graphs.

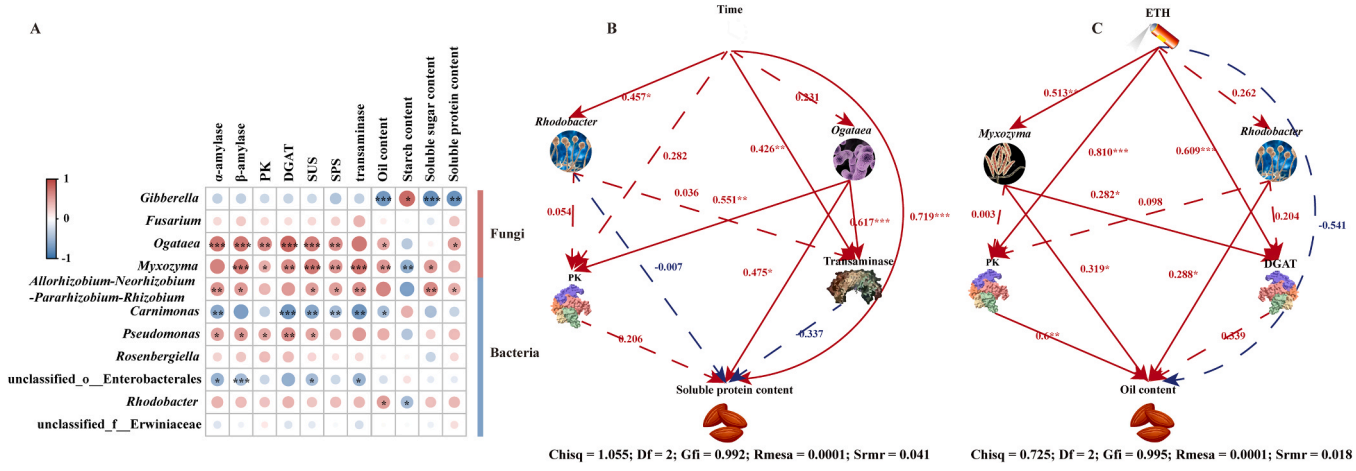

Fig. 4. Relationships between bacterial/ fungal genera and nut nutrients/ nut enzyme activities (A). Structural equation models (SEMs) showing the effects of time (B) and ethephon (C) on nut nutrients through nut microorganism and nut enzymes. Numbers adjacent to arrows are path coefficients. Continuous or dashed lines indicate significant or insignificant relationships. Red and blue arrows indicate positive and negative correlations, respectively. * $P < 0.05$; ** $P < 0.01$; ***$P < 0.001$.

ripening time were phyla Bacteroidota and Proteobacteria, class Bacteroidia, Gammaproteobacteria, Alphaproteobacteria, alongside 6 types of specific genera biomarkers, *Chryseobacterium*, unclassified_f_Weeksellaceae, *Rosenbergiella*, *Acetobacter*, *Pseudomonas*, *Gluconobacter*. At day 15 of ripening time, there were 3 species groups under both CK and ETH treatment that played major indictors roles, including genera *Dokdonella*, unclassified_f_Xanthomonadacee, and norank_f_norank_o_Rhodospirillales (Figs. 3C and 3E). For fungi, the specific biomarkers under ETH treatment included class Sordariomycetes and Dothideomycetes at day 5, with 3 types of specific genera biomarkers, *Fusarium*, *Cladosporium*, and *Ogataea* (Fig. 3F). The same biomarker under both CK and ETH treatments at day 10 was *Neopestalotiopsis*, whereas, biomarker at day 15 of the post-ripening stage was genus *Chalara*.

3.4. Linkages among nut microbiome, enzyme activity, and nut nutrients

To elucidate which microbes play important roles in nutrient conversion for nut during the post-ripening stage, correlations were analyzed between the relative abundance of 11 genera (enriched both in heat map and LEfSe analyses) and the macronutrients, nut enzyme activities (Fig. 4A). Positive relations in *Gibberella*, *Carnimonas*, and unclassified_O_Enterobacterales with starch content, while these genera were negatively correlated with activities of all nut enzymes, oil content, soluble sugar content, and soluble protein content. Contrary to the above genera, the genus *Ogataea*, *Myxozyma*, *Allorhizobium-Neorhizonium-Pararhizobium-Rhizobium, Pseudomonas* and *Rhodobacter* were positively correlated with nut enzyme activities and macronutrients, except for starch content. *Fusarium* and *Rosenbergiella* were negatively correlated to soluble sugar content. The genus *Ogataea* was positively associated with nut enzyme activities ($P<0.05$).

Moreover, SEM provided good fits to the data (Chisq=1.055, Df=2, Gfi=0.992, RMSEA=0.0001, Srmr=0.041 for soluble protein content; Chisq=0.725, Df=2, Gfi=0.995, RMSEA=0.0001, Srmr=0.018 for oil content) (Figs. 4B and 4C). According to the model, nut soluble protein content was directly influenced by post-ripening time, with the fungus *Ogataea* to exert a strong direct effect to protein level (Fig. 4B). ETH treatment appeared to affect nut oil content via its impact on fungi *Myxozyma* and enzyme PK (Fig. 4C).

3.5. Shifts in diversity and fungal functional associations of microbial community of T. grandis nut

For bacteria, the Ace index under CK treatment was kept stable from day 0 till day 15, whereas under ETH treatment was sustained from day 0 till day 10, with an increase from day 10 till 15 (Fig. 5A). In case of fungi, both the Ace index under CK and ETH treatment showed an increasing trend during the post-ripening stage (Fig. 5B). The bacterial and fungal community under CK at day 5 and day 10 were well separated from those at day 15 of post-ripening stage (Fig. S4A and S4B). Under ETH treatment, a distinct separation was observed among different post-ripening times and proving the impact of ETH on nut microbiome. The β diversity of bacteria under ETH showed clear discrimination from CK during the whole post-ripening stage (Fig. S4A), whereas a separation in β diversity of fungi was observed between CK and ETH groups only at day 10 (Fig. S4B).

The relative abundances of several functional guild differed among treatments (Fig. 5C). Compared with CK, ETH treatment had a higher relative abundance of undefined saprotroph from day 5 till day 10. To identify pathogen factor, fungi with relative abundance greater than 1 % were selected, including genera *Botryosphaeria*, *Chalara*, *Cladosporium*, *Fusarium*, *Gibberella*, *Lasiodiplodia*, and *Pestalotiopsis* (Fig. S5). Overall, *Chalara* was found strongly correlated with decay incidence with Mantel's r=0.655 and P=0.001 (Fig. 5D). While other potentially pathogenic fungi showed a negative correlation with decay incidence.

4. Discussion

4.1. Enhanced quality of T. grandis nut post ETH treatment

Starch, as the primary storage carbohydrate in seeds provides raw materials and energy for protein and oil synthesis (Dussert et al., 2013). In nuts, such as walnuts (*Juglans regia*), peanuts (*Arachis hypogaea*), oil content serves as a vital indicator in quality evaluation (Poggetti et al., 2017; Huang et al., 2022). Ethylene gas treatment has been shown to improve the quality of crude palm oil by improving oxidative stability and reducing bleaching index (Chew et al., 2021). In the present study, the decline in starch content under ETH treatment occurred more rapidly than under CK during day 5 till day 10 of the post-ripening stage, accompanied by higher oil contents (Fig. 1). In addition, PCA revealed a negative correlation between starch content and oil, soluble sugar, and protein contents (Fig. S1E). Chaudhari et al. (2023) demonstrated that the addition of ethylene enhances the activities of α-amylase and β-amylase and diacylglycerol acyltransferase (DGAT), which play crucial role in oil biosynthesis (Yang et al., 2016), and to account for the decline in starch level in *T. grandis* nuts. Similarly, the positive relationship between PK, DGAT and oil content may explain why ethylene addition increased nut oil content (Table1 and Fig. S2). Our previous study showed that the oil content of *T. grandis* attained its peak at 16 d when the postharvest period is completed (Zhang et al., 2020). In this study, the oil content under ETH treatment reached its peak at day 10, indicating that the post-ripening period is completed within 10 days.

Moreover, our study aligns with previous studies showing that decay incidences increase with longer storage periods (Zhang et al., 2021a; Li et al., 2022). However, ethylene plays a vital role in activating signaling pathways related to the host defense response to necrotrophic pathogens (Baró-Montel et al., 2020). This may explain the lower decay incidence observed under ETH treatment in our study compared with CK treatment (Fig. 1F). Altogether, ETH treatment appears beneficial for enhancing the postharvest quality of *T. grandis* nuts.

4.2. Microbial communities in relation to nut quality during the post-ripening stage

The bacterial and fungal microbiomes play a vital role in fruit nutrient conversion, maintaining nut postharvest quality (Zhang et al., 2021a; Zhimo et al., 2021; Perato et al., 2022). In this study, nuts under ETH treatment exhibited a higher relative abundance of *Allorhizobium-Neorhizobium-Pararhizobium-Rhizobium, Novosphingobium, Pseudomonas and Rosenbergiella*, with a decreased relative abundance of *Carnimonas*, especially during day 5 till day 10 (Fig. 3A). Moreover, four genera (including *Allorhizobium-Neorhizobium-Pararhizobium-Rhizobium, Pseudomonas, Rosenbergiella* and *Carnimonas*) were identified as bacterial biomarkers under ETH treatment by LEfSe analysis (Fig. 3E). *Carnimonas*, a bacterial genus topically found in salted foods, is known to cause black spots on food surface (Garriga et al., 1998; Arnau and Garriga, 2000). In contrast, *Pseudomonas* has been shown to strongly inhibit collar and root rot pathogen (Latha et al., 2011). In comparison with CK, the relative abundance of *Carnimonas* was lower under ETH treatment, whereas *Pseudomonas* increased during the whole post-ripening stage. Our study revealed that *Rosenbergiella* showed a negative correlation with soluble sugar content (Fig. 4A), and in accordance with previous reports that high sugar concentrations limit the growth of *Rosenbergiella* (Morales-Poole et al., 2022). *Allorhizobium-Neorhizobium-Pararhizobium-Rhizobium* is a key player in the biocatalytic upgrading of heavy crude oil (Raheem et al., 2022). This genus was positively correlated with oil content and negatively correlated with starch content (Fig. 4A). *Rhodobacter*, a genus of purple non-sulfur photosynthetic bacteria, can utilize starch and short chain fatty acids (SCFAs) to produce hydrogen and accumulate lipids (Assawamongkholsiri et al., 2016; Laurinavichene et al., 2017). Importantly, *Rhodobacter* was positively correlated with oil content, and SEM analysis confirmed its positive

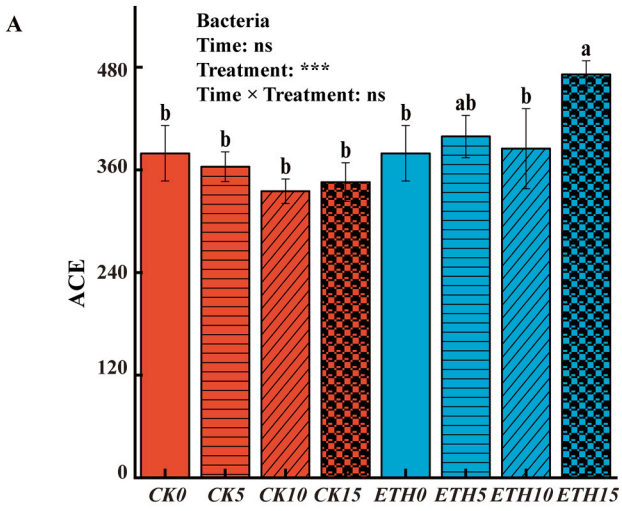

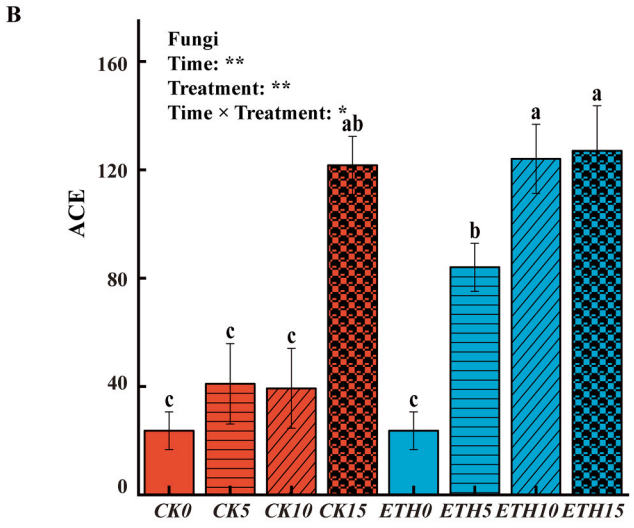

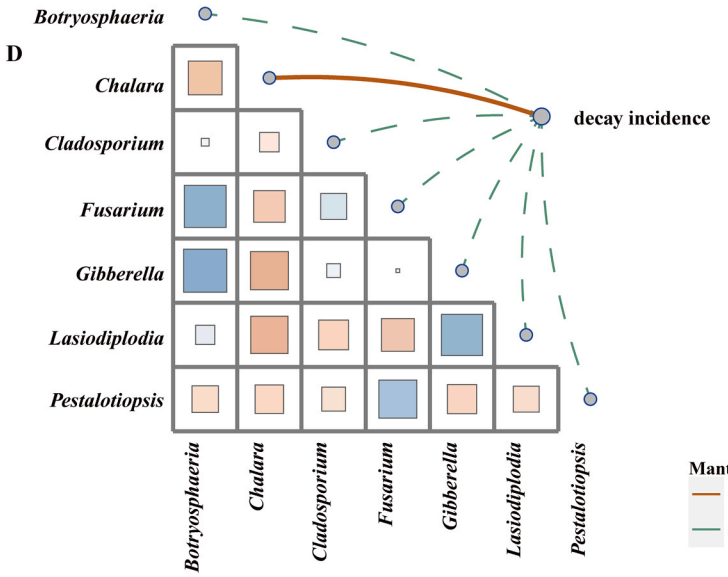

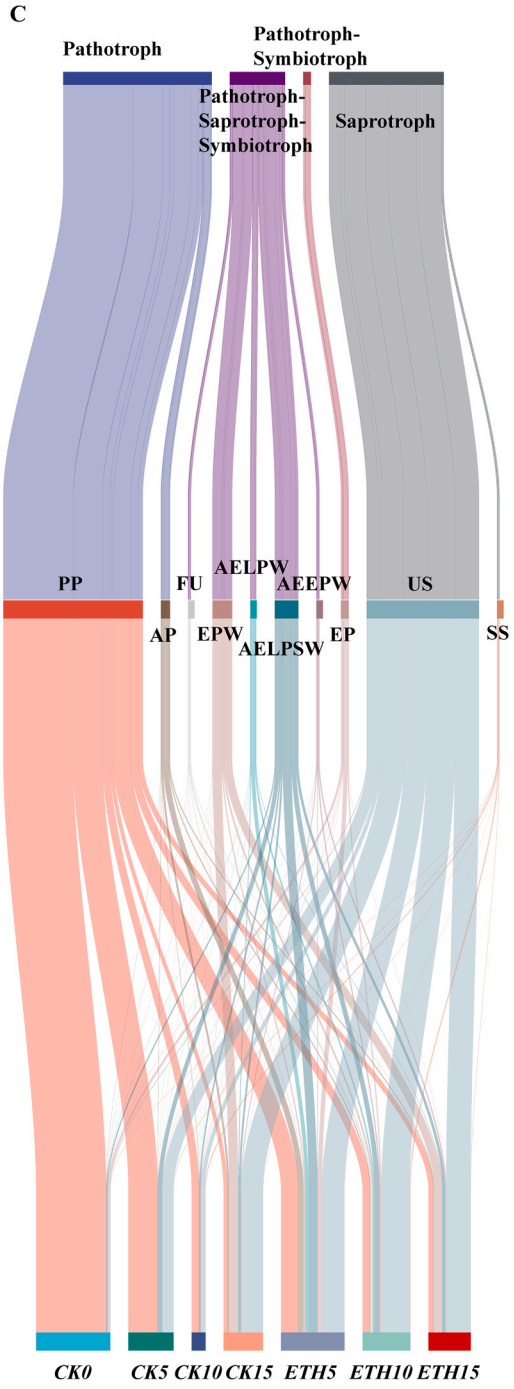

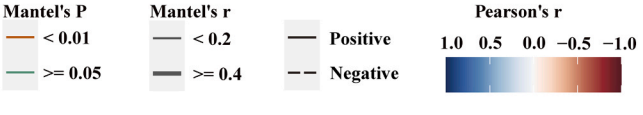

(caption on next page)

Fig. 5. The diversity and metabolism of nut microbial communities in CK and ethylene (ETH). Alpha diversity of bacterial (A) and fungal (B) communities. The Sankey diagram displays the top 10 functional guilds and their relative abundance (C). Correlations between potential pathogenic fungal genera and nut decay incidence determined using the Mantel test (D). Time, post-ripening stage; Treatment, different post-harvest treatments effect; Time× Treatment, interaction between post-ripening stage and different post-harvest treatments effect; ns, $P > 0.05$; * $P < 0.05$; ** $P < 0.01$. The color of the line represents the significance of the differences (P values), and the size of the line represents the correlation coefficients (Mantel's r). Pairwise correlations of these variables are shown with a color gradient representing the Spearman correlation coefficient. PP, Plant Pathogen. US, Undefined Saprotroph. AELPSW, Animal Pathogen-Endophyte-Lichen Parasite-Plant Pathogen-Soil Saprotroph-Wood Saprotroph. EPW, Endophyte-Plant Pathogen-Wood Saprotroph. AP, Animal Pathogen. EP, Endophyte-Plant Pathogen. AELPW, Animal Pathogen-Endophyte-Lichen Parasite-Plant Pathogen-Wood Saprotroph. AEEPW, Animal Pathogen-Endophyte-Ericoid Mycorrhizal-Plant Pathogen-Wood Saprotroph. FU, Fungal Parasite-Undefined Saprotroph. SS, Soil Saprotroph.

effect on nut oil accumulation (Fig. 4C). Thus, the higher relative abundance of *Rhodobacter* under ETH treatment may enhance oil biosynthesis in nuts during the post-ripening stage. Additionally, the increased relative abundance of *Pseudomonas* concurrent with the decreased relative abundance of *Carnimonas* may contribute to the lower decay incidence observed.

For fungi, the genera *Fusarium*, *Gibberella*, *Myxozyma*, *Ogataea*, and *Zygoascus* had higher relative abundance under ETH treatment than CK, and also acting as biomarkers under ETH treatment (except for *Zygoascus*) (Figs. 3B and 3F). The genus *Ogataea* is an industrial yeast known for protein production (Ye et al., 2023), which aligns with our study that *Ogataea* was positively correlated with soluble protein content (Figs. 4A and 4B). In addition, *Myxozyma* also functions as a superior lipid producing yeast (Dien et al., 2016), and its relative abundance under ETH treatment increased during day 5 till day 10 in comparison to CK (Fig. 3B). Moreover, SEM analysis further demonstrated that *Myxozyma* had a direct impact on oil content (Fig. 4C), and in accordance with Berikten (2023) report that oleaginous yeasts (e.g., *Myxozyma*) have the capacity to store lipids inside their cells, and overexpress DGAT enzyme to ultimately increase triacylglycerol accumulation. The fungal *Gibberella* is known for producing gibberellins, which regulate several plant developmental processes, for example, seed germination and fruit formation (Keswani et al., 2021), which might account for the decreasing trend of *Gibberella* abundance during the post-ripening period (Fig. 3B and Fig. S5). Although *Fusarium* is often considered as a fungal plant pathogen (Dean et al., 2012), many *Fusarium* species are used industrially for mycoprotein production (Bourdichon et al., 2012). For example, *Fusarium domesticum* is used in cheese fermentation (Bachmann et al., 2005). Consistent with our study, *Fusarium* was negatively correlated with decay incidence, but positively related to nut oil and soluble protein content (Fig. 4A and Fig. 5D). Altogether, the higher relative abundance of *Ogataea* and *Myxozyma* under ETH treatment may contribute to the enhanced nutrient conversion rate in nuts.

4.3. Correlation analysis of microbial communities and nut decay during the post-ripening stage

Nut decay is often caused by fungal pathogens, such as *Fusarium* (Zhang et al., 2021a), *Colletotrichum* (Li et al., 2022), and *Aspergillus* (Rodrigues et al., 2012; Morgan et al., 2020). In contrast, *Acremonium strictum* Elicitor Subtilisin has been shown to prevent fruit decay and improve postharvest quality in strawberry fruit by inducing ethylene production (Perato et al., 2022). In our study, ETH treatment resulted in low decay incidence during the post-ripening stage (Fig. 1F) suggestive to be mediated mostly via targeting microbial community.

Previous studies have highlighted the importance of microbial diversity in maintaining soil and plant health (Zhimo et al., 2021; Yu et al., 2022). Our results demonstrated that both ripening time and ETH treatment impacted α and β diversity of microbial communities during the post-ripening stage (Fig. 5 and Fig. S4). This is consistent with previous findings that both ethylene alongside postharvest ripening time strongly influence microbial community (Xie et al., 2021). Numerous studies have shown that high fungal and bacterial α-diversity is associated with reduced strawberry and sweet cherries rot incidence (Zhang et al., 2021b; Zhimo et al., 2021). This could explain why ETH treatment increased fungal α diversity was associated with lower decay incidence (Fig. 5). Furthermore, PCA revealed that bacterial and fungal communities were influenced by both the ethylene micro-environment and postharvest storage (Fig. S4A and S4B). Similar results were reported in kiwifruit with ethylene treatment (Xie et al., 2021).

Microbes with high abundance play critical roles in shaping the functional pattern of the entire microbial flora (Zhimo et al., 2021). To identify candidate pathogens responsible for decay in *T. grandis* nuts, the primary pathotroph fungal genera were selected according to Funguild results (Fig. 5C). Mantel analysis revealed that the genus *Chalara* was positively related with nut decay incidence (Fig. 5D). Approximately 60 % of the top fungal pathogens belong to phylum Ascomycota (Bansal et al., 2022). In the present study, Ascomycota was the major phylum (account for 88 %-96 % of the fungal community) and the fungi *Chalara* was part of this phylum (Fig. S3C and Fig. S3D). Similar results were reported by Suleman et al. (2007) and Michel (2009) revealing that *Chalara paradoxa*, *Chalara radicicola* and *Chalara elegans* are plant pathogen. Thus, we can infer that nut decay in *T. grandis* is mostly associated with the fungus *Chalara*, and that ETH treatment reduces the relative abundance of this genus leading to decreased decay incidence.

Therefore, ETH treatment enhanced *T. grandis* nut quality by altering the microbial community composition via two main targets as summarized in (Fig. 6): 1) through direct and indirect effects, such as influencing the activity of PK and DGAT enzymes, the beneficial genera *Rhodobacter* and *Myxozyma* contributing to the oil content reaching its peak on the 10th day of the post-ripening stage. 2) lower relative

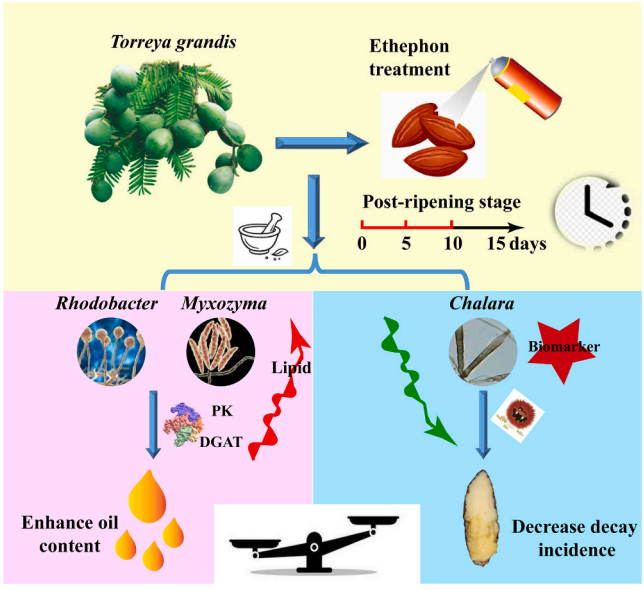

Fig. 6. The conceptual figure illustrates that the effect of ethylene shortens the post-ripening time and improves nut quality by altering the microbial community during the post-ripening stage. Specifically, ethephon treatment increases its oil content by enhancing the number of beneficial microbes (*Rhodobacter* and *Myxozyma*) and the activity of nutrient transformation enzymes (PK and DGAT). Additionally, it reduced nut decay incidence by decreasing the abundance of pathogen *Chlara*.

abundance of *Chalara* to reduce decay incidence, acting as a fungal biomarker for nut decay.

5. Conclusion

This study indicates that the addition of ethylene reduced the post-ripening stage to 10 days and decreased decay incidence in *T. grandis*. We demonstrated that ethylene application led to substantial alterations in the bacterial and fungal communities, including changes in both diversity and composition. ETH treatment increased nut oil content mainly via affecting the relative abundance of the genera *Myxozyma* and *Rhodobacter*, as well as enhancing enzyme PK activity. The fungal genus *Chalara*, was found to be correlated with nut decay incidence and exhibited lower relative abundance under ETH treatment. Therefore, improved quality and reduced decay incidence of *T. grandis* nuts with ETH treatment were closely associated with changes in microbial community structure. These results highlight the dynamic relationship between the microbial community and *T. grandis* nuts quality during the post-ripening stage. The underlying mechanisms identified from this study can be further exploited to improve nut quality in the future.

Author Statement Contributions

Suo J.W., Zhou Z.H. contributed equally to the conceptualization of the study, methodology design, data analysis, and manuscript writing. Suo J.W., Zhou Z.H., Hu Y.Y. was responsible for experimental execution and data collection. Wu J.S., Hu Y.Y., Song L.L. provided critical revisions and contributed to the interpretation of results. All authors reviewed and approved the final manuscript.

CRediT authorship contribution statement

Jinwei Suo: Writing – original draft, Methodology, Data curation, Conceptualization. **Mohamed Ali Farag:** Writing – review & editing. **Zhanhua Zhou:** Writing – original draft, Data curation, Conceptualization. **Jiasheng Wu:** Writing – review & editing. **Zuying Zhang:** Writing – review & editing. **Lili Song:** Writing – review & editing, Supervision. **Yuan Hu:** Writing – review & editing, Resources, Investigation.

Declaration of Competing Interest

The authors declare that they have no known competing financial interests or personal relationships that could have appeared to influence the work reported in this paper.

Acknowledgements

This work was financially supported by the National Natural Science Foundation of China (U23A20219; 32271922; 32001349; 32101556), the National Key Research and Development Program of China (2022YFD2200603); R&D Project of National Forest and Grass Machinery Sci-Tech Innovation Park (2023YG10), the Selective Breeding of New Cultivars in T. grandis (2021C02066–11), and the 111 Project (D18008)

Appendix A. Supporting information

Supplementary data associated with this article can be found in the online version at doi:10.1016/j.postharvbio.2024.113250.

Data availability

Data will be made available on request.

References

Aguilar, C.N., Rodríguez, R., Gutiérrez-Sánchez, G., Augur, C., Contreras-Esquivel, J.C., 2007. Microbial tannases: advances and perspectives (https://doi.). Appl. Microbiol. Biot. 76, 47–59. https://doi.org/10.1007/s00253-007-1000-2.

Arnau, J., Garriga, M., 2000. The effect of certain amino acids and browning inhibitors on the 'black spot' phenomenon produced by *Carnimonas nigrificans*. J. Sci. Food Agr. 80, 1655–1658. https://doi.org/10.1002/1097-0010(20000901)80:11<1655::AID-JSFA701>3.0.CO;2-M.

Assawamongkholsiri, T., Plangklang, P., Reungsang, A., 2016. Photofermentaion and lipid accumulation by *Rhodobacter* sp. KKU-PS1 using malic acid as a substrate. Int. J. Hydrog. Energ. 41, 6259–6270. https://doi.org/10.1016/j.ijhydene.2016.02.118.

Bachmann, H.P., Bobst, C., Bütikofer, U., Casey, M.G., Torre, M., Frhlich-Wyder, M.T., Fürst, M., 2005. Occurrence and significance of *Fusarium domesticum* alias *Anticollanti* on smear-ripened cheeses (https://doi.). LWT - Food Sci. Technol. 38, 399–407. https://doi.org/10.1016/j.lwt.2004.05.018.

Bansal, S., Mallikarjuna, M.G., Balamurugan, A., Nayaka, S.C., Prakash, G., 2022. Composition and codon usage pattern results in divergence of the *Zinc binuclear cluster* ($Zn(II)_2Cys_6$) sequences among ascomycetes plant pathogenic fungi (https://doi.org/). J. Fungi 8, 1134. https://doi.org/10.3390/jof8111134.

Baró-Montel, N., Giné-Bordonaba, J., Torres, R., Vall-Llaura, N., Teixidó, N., Usall, J., 2020. Scrutinising the relationship between major physiological and compositional changes during 'Merrill O'Henry' peach growth with brown rot susceptibility (https://doi.org/). Food Sci. Technol. Int. 27, 366–379. https://doi.org/10.1177/1082013220959988.

Berikten, D., 2023. Oleaginous yeasts: phylogenetic diversity and strain selection for biodiesel production. Advances in yeast biotechnology for biofuels and sustainability. Elsevier Inc, pp. 117–138.

Bourdichon, F., Casaregola, Serge, Farrokh, C., Frisvad, J.C., Gerds, M.L., Hammes, W.P., Harnett, J., Huys, G., Laulund, S., Ouwehand, A., Powell, I.B., Prajapati, J.B., Seto, Y., Schure, E.T., Boven, A.V., Vankerckhoven, V., Zgoda, A., Tuijtelaars, S., Hansen, E.B., 2012. Food fermentations: microorganisms with technological beneficial use (https://doi.). Int. J. Food Microbiol. 154, 87–97. https://doi.org/10.1104/pp.113.220525.

Chaudhari, H.A., Mahatma, M.K., Antala, V., Radadiya, N., Ukani, P., Tomar, R.S., Thawait, L.K., Singh, S., Gangadhara, K., Sakure, A., Parihar, A., 2023. Ethrel-induced release of fresh seed dormancy causes remodelling of amylase activity, proteomics, phytohormone and fatty acid profile of groundnut (*Arachis hypogaea* L.) (https://doi.org/). Physiol. Mol. Biol. Pla. 29, 829–842. https://doi.org/10.1007/s12298-023-01332-6.

Chew, C.L., Tan, B.A., Low, J.Y.S., Hakimi, N.I.N.M., Kua, S.F., Lim, C.M., 2021. Exogenous ethylene application on postharvest oil palm fruit bunches improves crude palm oil quality (https://doi.). Food Sci. Nutr. 9, 5335–5343. https://doi.org/10.1002/fsn3.2423.

Dean, R., Van Kan, J.A.L., Pretorius, Z.A., Hammond-Kosack, K.E., Di Pietro, A., Spanu, P.D., Rudd, J.J., Dickman, M., Kahmann, R., Ellis, J., Foster, G.D., 2012. The top 10 fungal pathogens in molecular plant pathology (https://doi.org/). Mol. Plant Pathol. 13, 414–430. https://doi.org/10.1111/j.1364-3703.2011.00783.x.

Dien, B.S., Slininger, P.J., Kurtzman, C.P., Moser, B.R., O'Bryan, P.J., 2016. Identification of superior lipid producing *Lipomyces* and *Myxozyma* yeasts (https://doi.). AIMS Environ. Sci. 3, 1–20. https://doi.org/10.3934/environsci.2016.1.1.

Dussert, S., Guerin, C., Andersson, M., Joet, T., Tranbarger, T.J., Pizot, M., Sarah, G., Omore, A., Durand-Gasselin, T., Morcillo, F., 2013. Comparative transcriptome analysis of three oil palm fruit and seed tissues that differ in oil content and fatty acid composition (https://doi.). Plant Physiol. 162, 1337–1358. https://doi.org/10.1104/pp.113.220525.

García-Ayuso, L.E., Velasco, J., Dobarganes, M.C., Luque de Castro, M.D., 2000. Determination of the oil content of seeds by focused microwave-assisted soxhlet extraction (https://doi.). Chromatographia 52, 103–108. https://doi.org/10.1007/bf02490801.

Garriga, M., Ehrmann, M.A., Arnau, J., Hugas, M., Vogel, R.F., 1998. Carnimonas nigrificans gen. nov., sp. nov., a bacterial causative agent for black spot formation on cured meat products (https://doi.org/). Int. J. Syst. Bacteriol. 48, 677–686. https://doi.org/10.1099/00207713-48-3-677.

Han, X., Shen, C., He, F., Liu, Y., Luo, Z., 2024. Potential regulator of ethylene and ABA in aroma recovery of kiwifruit after transferring from cold storage (https://doi.org/). Sci. Hortic. 335, 113343. https://doi.org/10.1016/j.scienta.2024.113343.

Hu, S., He, C., Li, Y., Yu, Z., Chen, Y., Wang, Y., Ni, D., 2021. Changes of fungal community and non-volatile metabolites during pile-fermentation of dark green tea. Food Res. Int. 147, 110472. https://doi.org/10.1016/j.foodres.2021.110472.

Hu, Y., Zhang, Z., Hua, B., Tao, L., Chen, W., Gao, Y., Suo, J., Yu, W., Wu, J., Song, L., 2022. The interaction of temperature and relative humidity affects the main aromatic components in postharvest *Torreya grandis* nuts. Food Chem. 368, 130836. https://doi.org/10.1016/j.foodchem.2021.130836.

Huang, X., Hong, M., Meng, Q., Zhang, Y., Kou, X., Ke, Q., 2024. The effects of core microorganism community on flavor compounds and active substances during the aging process of *Citri Reticulatae* Pericarpium. Food Res. Int. 191, 114707. https://doi.org/10.1016/j.foodres.2024.114707.

Huang, Y., Liu, C., Huang, F., Zhou, Q., Zheng, C., Liu, R., Huang, J., 2022. Quality evaluation of oil by cold-pressed peanut from different growing regions in China (https://doi.). Food Sci. Nutr. 10, 1975–1987. https://doi.org/10.1002/fsn3.2813.

Keswani, C., Singh, S.P., García-Estrada, C., Mezaache-Aichour, S., Glare, T.R., Borriss, R., Rajput, V.D., Minkina, T.M., Ortiz, A., Sansinenea, E., 2021. Biosynthesis and beneficial effects of microbial gibberellins on crops for sustainable agriculture. J. Appl. Microbiol. 132, 1597–1615. https://doi.org/10.1111/jam.15348.

Lane, C., Al Shoffe, Y., Schafran, P., Li, F.-W., Kao-Kniffin, J., Watkins, C.B., 2024. Amplicon sequencing and shotgun metagenomics reveal functional impacts of aminoethoxyvinylglycine-mediated ripening and cold storage on the microbiome of 'NY1' apples. Postharvest Bio. Tec. 213, 112969. https://doi.org/10.1016/j.postharvbio.2024.112969.

Latha, P., Anand, T., Prakasam, V., Jonathan, E.I., Paramathma, M., Samiyappan, R., 2011. Combining *Pseudomonas*, *Bacillus* and *Trichoderma* strains with organic amendments and micronutrient to enhance suppression of collar and root rot disease in physic nut. Appl. Soil. Ecol. 49, 215–223. https://doi.org/10.1016/j.apsoil.2011.05.003.

Laurinavichene, T., Laurinavichius, K., Shastik, E., Tsygankov, A., 2017. Long-term H2 photoproduction from starch by co-culture of *Clostridium butyricum* and *Rhodobacter sphaeroides* in a repeated batch process. Biotechnol. Lett. 40, 309–314. https://doi.org/10.1007/s10529-017-2486-z.

Lefcheck, J.S., 2015. piecewiseSEM: Piecewise structural equation modelling in R for ecology, evolution, and systematics. Methods Ecol. Evol. 7, 573–579. https://doi.org/10.1111/2041-210x.12512.

Li, M., Yang, S., Peng, L., Zeng, K., Feng, B., Jingjing, Y., 2022. Compositional shifts in fungal community of chestnuts during storage and their correlation with fruit quality. Postharvest Bio. Tec. 191, 111983. https://doi.org/10.1016/j.postharvbio.2022.111983.

Li, Z., Dai, W., 2007. Chinese Torreya. Chinese Torreya. Science Press Beijing.

Maduwanthi, S.D.T., Marapana, R.A.U.J., 2021. Comparison of pigments and some physicochemical properties of banana as affected by ethephon and acetylene induced ripening. Biocatal. Agric. Biotechnol. 33, 101997. https://doi.org/10.1016/j.bcab.2021.101997.

Michel, V.V., 2009. First report of *Chalara elegans* on roots of black elderberry. Plant Dis. 93, 963. https://doi.org/10.1094/pdis-93-9-0963a.

Morales-Poole, J.R., de Vega, C., Tsuji, K., Jacquemyn, H., Junker, R.R., Herrera, C.M., Michiels, C., Lievens, B., Álvarez-Pérez, S., 2022. Sugar concentration, nitrogen availability, and phylogenetic factors determine the ability of *Acinetobacter* spp. and *Rosenbergiella* spp. to grow in floral nectar. Microb. Ecol. 86, 377–391. https://doi.org/10.1007/s00248-022-02088-4.

Morgan, vH.A., Thie, I.B., Pedro, A.N.D., de, R.J.B., Manoel, M.L., Hiromi, T.M., Silva, N. M., 2020. Interaction of *Aspergillus flavus* and *A. parasiticus* with *Salmonella* spp. isolated from peanuts. Int. J. Food Microbiol. 328, 108666. https://doi.org/10.1016/j.ijfoodmicro.2020.108666.

Perato, S.M., Furio, R.N., Tomas-Grau, R.H., Salazar, S.M., Díaz Ricci, J.C., Martinez-Zamora, M.G., 2022. AsES elicitor induces ethylene production, accelerates ripening, and prevents *Botrytis cinerea* rot in strawberry fruit. Eur. J. Plant Pathol. 164, 229–239. https://doi.org/10.1007/s10658-022-02553-3.

Poggetti, L., Ferfuia, C., Chiabà, C., Testolin, R., Baldini, M., 2017. Kernel oil content and oil composition in walnut (*Juglans regia* L.) accessions from North Eastern Italy. J. Sci. Food Agr. 98, 955–962. https://doi.org/10.1002/jsfa.8542.

Raheem, A.S.A., Hentati, D., Bahzad, D., Abed, R.M.M., Ismail, W., 2022. Biocatalytic upgrading of unconventional crude oil using oilfield-inhabiting bacterial consortia. Int. Biodeter. Biodegr. 174, 105468. https://doi.org/10.1016/j.ibiod.2022.105468.

Read, S.M., Northcote, D.H., 1981. Minimization of variation in the response to different proteins of the coomassie blue G dye-binding assay for protein. Anal. Biochem. 116, 53–64.

Rodrigues, P., Venâncio, A., Lima, N., 2012. Mycobiota and mycotoxins of almonds and chestnuts with special reference to aflatoxins. Food Res. Int. 48, 76–90. https://doi.org/10.1016/j.foodres.2012.02.007.

Roze, L.V., Calvo, A.M., Gunterus, A., Beaudry, R., Kall, M., Linz, J.E., 2004. Ethylene modulates development and toxin biosynthesis in *Aspergillus* possibly via an ethylene sensor–mediated signaling pathway (https://doi.). J. Food Prot. 67, 438–447. https://doi.org/10.4315/0362-028x-67.3.438.

Shi, Y., Yang, Q., Zhao, Q., Dhanasekaran, S., Ahima, J., Zhang, X., Zhou, S., Droby, S., Zhang, H., 2021. *Aureobasidium pullulans* S-2 reduced the disease incidence of tomato by influencing the postharvest microbiome during storage. Postharvest Bio. Tec. 185, 111809. https://doi.org/10.1016/j.postharvbio.2021.111809.

Suleman, P., Al-Musallam, A., Menezes, C.A., 2007. The effect of solute potential and water stress on black scorch caused by *Chalara paradoxa* and *Chalara radicicola* on date palms. Plant Dis. 85, 80–83. https://doi.org/10.1094/pdis.2001.85.1.80.

Sun, X., Zhang, X., Zhang, G., Miao, Y., Zeng, T., Zhang, M., Zhang, H., Zhang, L., Huang, L., 2022. Environmental response to root secondary metabolite accumulation in *Paeonia lactiflora*: Insights from rhizosphere metabolism and root-associated microbial communities. Microbiol. Spectr. 10, 1–20. https://doi.org/10.1128/spectrum.02800-22.

Suo, J., Gao, Y., Zhang, H., Wang, G., Cheng, H., Hu, Y., Lou, H., Yu, W., Dai, W., Song, L., Wu, J., 2022. New insights into the accumulation of vitamin B_3 in *Torreya grandis* nuts via ethylene induced key gene expression. Food Chem. 371, 131050. https://doi.org/10.1016/j.foodchem.2021.131050.

Suo, J., Tong, K., Wu, J., Ding, M., Chen, W., Yang, Y., Lou, H., Hu, Y., Yu, W., Song, L., 2019. Comparative transcriptome analysis reveals key genes in the regulation of squalene and β-sitosterol biosynthesis in *Torreya grandis*. Ind. Crop. Prod. 131, 182–193. https://doi.org/10.1016/j.indcrop.2019.01.035.

Tian, L., Wang, L., 2020. A meta-analysis of microbial community structures and associated metabolic potential of municipal wastewater treatment plants in global scope. Environ. Pollut. 263, 114598. https://doi.org/10.1016/j.envpol.2020.114598.

Tovar, B., Montalvo, E., Damián, B.M., García, H.S., Mata, M., 2011. Application of vacuum and exogenous ethylene on Ataulfo mango ripening. LWT - Food Sci. Technol. 44, 2040–2046. https://doi.org/10.1016/j.lwt.2011.06.005.

Wang, Q., Peng, C., Gong, J., 2011. Effects of enzymatic action on the formation of theabrownin during solid state fermentation of Pu-erh tea. J. Sci. Food Agr. 91, 2412–2418. https://doi.org/10.1002/jsfa.4480.

Wassermann, B., Kusstatscher, P., Berg, G., 2019. Microbiome response to hot water treatment and potential synergy with biological control on stored apples. Front. Microbiol. 10, 2502. https://doi.org/10.3389/fmicb.2019.02502.

Wu, J., Huang, J., Hong, Y., Zhang, H., Ding, M., Lou, H., Hu, Y., Yu, W., Song, L., 2018. *De novo* transcriptome sequencing of *Torreya grandis* reveals gene regulation in sciadonic acid biosynthesis pathway. Ind. Crop. Prod. 120, 47–60. https://doi.org/10.1016/j.indcrop.2018.04.041.

Wu, W., Lei, J., Hussain, M., Cao, S., Dui, B., Wang, R., 2019. Structure and function of the fruit microbiome in healthy and diseased kiwifruit. Pak. J. Agr. Sci. 56, 577–585. https://doi.org/10.21162/pakjas/19.8820.

Xie, Y., Nian, L., Zeng, Y., Wang, M., Yuan, B., Cheng, S., Cao, C., 2021. Dynamic variation of endogenous flora in kiwifruit and its association with ripening metabolism in response to ethylene micro-environment. Postharvest Bio. Tec. 182, 111695. https://doi.org/10.1016/j.postharvbio.2021.111695.

Yang, H., Ye, W., Yu, Z., Shen, W., Li, S., Wang, X., Chen, J., Wang, Y., Zheng, X., 2023. Host niche, genotype, and field location shape the diversity and composition of the soybean microbiome. J. Integr. Agr. 22, 2412–2425. https://doi.org/10.1016/j.jia.2023.01.006.

Yang, Z., Ji, H., Liu, D., 2016. Oil biosynthesis in underground oil-rich storage vegetative tissue: comparison of *Cyperus esculentus* tuber with oil seeds and fruits. Plant Cell Physiol. 57, 2519–2540. https://doi.org/10.1093/pcp/pcw165.

Ye, M., Gao, J., Zhou, Y.J., 2023. Global metabolic rewiring of the nonconventional yeast *Ogataea polymorpha* for biosynthesis of the sesquiterpenoid β-elemene. Metab. Eng. 76, 225–231. https://doi.org/10.1016/j.ymben.2023.02.008.

Yu, H., Tian, S., Huang, Q., Chen, J., Wu, Y., Wang, R., Lu, L., 2021. An insect- and rain-proof net raises the production and quality of chinese bayberry by preventing damage from insects and altering bacterial communities. Front. Plant Sci. 12, 732012. https://doi.org/10.3389/fpls.2021.732012.

Yu, L., Bai, J., Huang, L., Zhang, G., Wang, W., Wang, X., Yu, Z., 2022. Carbon-rich substrates altered microbial communities with indication of carbon metabolism functional shifting in a degraded salt marsh of the Yellow River Delta, China. J. Clean. Prod. 331, 129898. https://doi.org/10.1016/j.jclepro.2021.129898.

Zhang, Y., Gao, C., Masum, M.M.I., Cheng, Y., Wei, C., Guan, Y., Guan, J., 2021a. Dynamic microbiome changes reveal the effect of 1-methylcyclopropene treatment on reducing post-harvest fruit decay in "Doyenne du Comice" pear (https://doi.). Front. Microbiol. 12, 729014. https://doi.org/10.3389/fmicb.2021.729014.

Zhang, Q., Shi, W., Zhou, B., Du, H., Xi, L., Zou, M., Zou, H., Xin, L., Gao, Z., Chen, Y., 2021b. Variable characteristics of microbial communities on the surface of sweet cherries under different storage conditions (https://doi.). Postharvest Bio. Tec. 173, 111408. https://doi.org/10.1016/j.postharvbio.2020.111408.

Zhang, Z., Chen, W., Tao, L., Wei, X., Gao, L., Gao, Y., Suo, J., Yu, W., Hu, Y., Yang, B., Jiang, H., Farag, M.A., Wu, J., Song, L., 2022. Ethylene treatment promotes umami taste-active amino acids accumulation of *Torreya grandis* nuts post-harvest by comparative chemical and transcript analyses. Food Chem. 408, 135214. https://doi.org/10.1016/j.foodchem.2022.135214.

Zhang, Z., Jin, H., Suo, J., Yu, W., Zhou, M., Dai, W., Song, L., Hu, Y., Wu, J., 2020. Effect of temperature and humidity on oil quality of harvested *Torreya grandis* cv. Merrillii nuts during the after-ripening stage (https://doi.). Front. Plant Sci. 11, 573681. https://doi.org/10.3389/fpls.2020.573681.

Zheng, B., 2006. Modern plant physiology and biochemistry research technique. Modern plant physiology and biochemistry research technique. China Meteorological Press, Beijing.

Zhimo, V.Y., Kumar, A., Biasi, A., Salim, S., Feygenberg, O., Toamy, M.A., Abdelfattaah, A., Medina, S., Freilich, S., Wisniewski, M., Droby, S., 2021. Compositional shifts in the strawberry fruit microbiome in response to near-harvest application of *Metschnikowia fructicola*, a yeast biocontrol agent. Postharvest Bio. Tec. 175, 111469. https://doi.org/10.1016/j.postharvbio.2021.111649.